Contents lists available at ScienceDirect

Tribology International

Simulation of wear evolution using fictitious eigenstrains

Zupan Hu [a], Wei Lu [a], M.D. Thouless [a,b], J.R. Barber [a,*]

[a] Department of Mechanical Engineering, University of Michigan, Ann Arbor, MI 48109-2125, USA
[b] Department of Materials Science & Engineering, University of Michigan, Ann Arbor, MI 48109-2136, USA

A R T I C L E   I N F O

A B S T R A C T

A numerical algorithm is described in which changes of geometry caused by wear can be simulated by ascribing fictitious anisotropic eigenstrains to a set of surface nodes. These eigenstrains are related to the wear depth at any location, and can be incorporated into calculations using the existing expansion modules in commercial codes, such as anisotropic swelling or thermal expansion. The proposed algorithm has been implemented, and the results compared to those from a conventional wear model involving periodic re-meshing. It has been shown to be accurate and efficient. The method provides an alternative to the re-meshing technique, and may provide advantages in history-dependent problems such as those involving plasticity, hysteretic friction or micro-slip.

© 2014 Elsevier Ltd. All rights reserved.

1. Introduction

Wear is a cause of failure in many engineering applications [1–4]. Predictions of the magnitude and distribution of wear are crucial for safety, and for the determination of operational costs. The local wear rate depends on the contact pressure, and even relatively small amounts of wear can change the profiles of the contacting bodies sufficiently to have a significant influence on the distribution of contact pressures. The contact and wear problems are therefore fully coupled, and require an incremental formulation in numerical models.

1.1. Methods for wear modeling

The Euler scheme is commonly used for wear modeling [5–9]. At each time step, the contact tractions are determined based on the instantaneous geometry of the system, and the wear rate is determined from these tractions using a wear law such as that proposed by Archard [10]. The geometry is then updated to reflect the wear predicted at each node during the time step, and the process is repeated.

The geometry updating can be realized either by re-meshing or by alternative techniques such as adjusting the magnitude of gap elements to account for wear [11]. In principle, the geometry should be updated after each time step, but this can be prohibitively computer-intensive, particularly since contact problems typically require a relatively fine mesh in the contact area [12]. Instead, it is usual to solve the contact problem under the assumption that the undeformed profile remains unchanged for

an extended period of time. If the loading is periodic, the model is indexed through one complete loading cycle and the total wear predicted at each node is determined. This cyclic nodal wear is then multiplied by an appropriate factor n to approximate the wear during a macro-time step of n loading cycles, after which the geometry of the contacting bodies is updated appropriately. The size of the macro-time step can be adjusted so as to ensure that the nodal wear is large enough to be numerically significant, but not so large as to introduce significant errors [6,13,14].

Soderberg and Andersson [7] found that frequent mesh adjustments can induce stability problems, and may increase the difficulty of numerical convergence. For example, they found that the adjustment of nodal coordinates may result in a spurious gap at some nodes, necessitating the repositioning of contact components, which introduces additional uncertainty into the accuracy of the results. Techniques have also been developed to improve the stability of the models when the wear depth is large compared to the element size [5]. For example, if the mesh adjustment is distributed among several layers of elements, the mesh quality can be preserved [14,15]. Both the re-meshing and multi-layer methods can effectively improve numerical stability, but they increase computational cost significantly.

In this paper, we present a new method in which the geometry is updated by imposing fictitious anisotropic eigenstrains (contractions) in the surface elements. The magnitude of these eigenstrains corresponds to the geometry change induced by wear. Several different modules exist in most commercial finite-element codes that can be used to induce anisotropic eigenstrains. These include swelling and thermal expansion modules. The use of these modules means that very little program modifications need to be made by the user, and avoids the need for re-meshing in cases of moderate wear. This is particularly useful for systems with a

Nomenclature		x	distance from the mid-point of the substrate along the interface
τ	shear traction at contact interface	w	wear depth
σ	normal traction (compressive positive) at contact interface	h	slip displacement
		α	wear coefficient
μ	friction coefficient	α_T	coefficient of thermal expansion
ν	Poisson's ratio	n	number of cycles between mesh geometry updates
E	Young's modulus	N	number of geometry updates
p	externally applied normal pressure	$\mathbf{W}$	vector of nodal displacements
d	amplitude of imposed tangential displacement	$\mathbf{T}$	vector of nodal temperatures
l	half length of the indenter and substrate	$\mathbf{\Delta}$	vector of eigenstrains
h	height of the indenter and height of the substrate		

dependence on loading history, such as elastic–plastic or Coulomb friction problems. Here, we describe the method, and validate it by using the thermal-expansion module in a commercial finite-element code to produce wear profiles from a simple example that can be compared to the results from a conventional re-meshing scheme.

2. Wear modeling by fictitious eigenstrains

The displacement of the surface nodes due to wear is realized by controlling the contraction of a layer of elements adjacent to the contact surface. These surface elements have the same material properties as the wearing material, but can undergo anisotropic contraction to mimic a wear profile. Fig. 1 shows a region of a finite-element mesh near the expected contact region, both in the undeformed condition, and as modified by wear defined through a vector of nodal displacements $\mathbf{W} = \{W_1, W_2, ..., W_m\}^T$, where m is the number of potential contact nodes. The required wear profile is achieved by assigning appropriate values to the corresponding m element eiegnstrains $\mathbf{\Delta} = \{\Delta_1, \Delta_2, ..., \Delta_m\}^T$. In order to avoid unwanted lateral displacements, so the simulated wear always occurs normal to the surface, the local orientations of the elements in contact are tracked by a subroutine at every time-step. The eigen-strains are set to be anisotropic, with only the components normal to the contact surface being non-zero. Therefore, contraction occurs only normal to the current, wear-modified contact surface.

In order to implement the method, we need to determine the relation between the vectors $\mathbf{W}$ and $\mathbf{\Delta}$. In ABAQUS, the nodal thermal displacement depends on the temperature of the neighboring nodes as well as that of the node itself, but in a linear model we can represent this relationship in the form

$$W_i = A_{ij}\Delta_j \quad \text{or} \quad \mathbf{W} = \mathbf{A}\mathbf{\Delta}, \tag{1}$$

where $i, j \in (1, m)$ and $\mathbf{A}$ is a matrix which depends only on the properties of the original finite-element model. In principle, $\mathbf{A}$ can be extracted from the finite-element code, using appropriate matrix operations [16]. However, an easier, though less elegant,
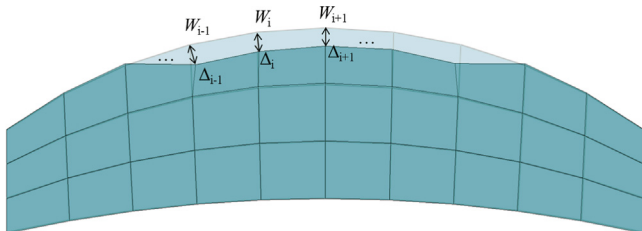

Fig. 1. The updating of the wear profile is realized through anisotropic eigenstrains in a layer of surface elements.

approach is to note that if no loads are applied and if the element eigenstrain vector is set to

$$\Delta_j = \delta_{kj} \tag{2}$$

where δ_{kj} is the Kronecker delta, the resulting nodal displacements will be

$$W_i = A_{ij}\delta_{kj} = A_{ik}. \tag{3}$$

Thus, a single run of the code with this eigenstrain distribution yields the coefficients A_{ik} with $i \in (1, m)$, which defines the kth row or column of $\mathbf{A}$. Repeating the operation m times for each value of k, we can construct the entire $m \times m$ matrix $\mathbf{A}$.

3. The Euler updating algorithm

We next embed the wear calculations in an Euler updating algorithm which is similar to that used with more conventional re-meshing methods. We assume Archard's wear law [10] in the form

$$\dot{w}(x, t) = \mu\alpha\dot{h}(x, t)p(x, t), \tag{4}$$

where μ is the coefficient of friction, α is the wear coefficient, $p(x, t)$ is the local contact pressure and $\dot{h}(x, t)$ is the slip velocity at the contact surface [$h(x, t)$ is the slip *displacement*]. The coefficient of friction is used in this formulation of Archard's law to emphasize that the wear rate is related to the contact stress through the frictional work done. In the finite-element model, the contact pressure and the wear rate are expressed in terms of nodal values $P_i(t), W_i(t)$ through the relations

$$\dot{p}(x, t) = \sum_{i=1}^{m} P_i(t)v_i(x), \quad \dot{w}(x, t) = \sum_{i=1}^{m} \dot{W}_i(t)v_i(x), \tag{5}$$

where $v_i(x)$ are the element-shape functions. It follows from (Eqs. (4) and 5) that

$$\dot{W}_i(t) = \mu\alpha\dot{H}_i(t)P_i(t), \tag{6}$$

where $\dot{H}_i(t)$ is the instantaneous slip velocity at node i. The nodal forces, $P_i(t)$, are determined by running the finite-element contact simulation through a complete loading cycle, after which Eq. (6) can be numerically integrated by dividing the loading cycle into appropriate time steps, Δt, and writing

$$W_i(t + \Delta t) = W_i(t) + \mu\alpha[H_i(t + \Delta t) - H_i(t)]P_i(t). \tag{7}$$

The resulting cyclic nodal wear is then multiplied by the factor n to determine the wear vector $\mathbf{W}$ after n cycles of loading. This is mathematically equivalent to the use of an enhanced wear rate $n\alpha$ in a single cycle of loading. The fictitious eigenstrain vector, $\mathbf{\Delta}$, is
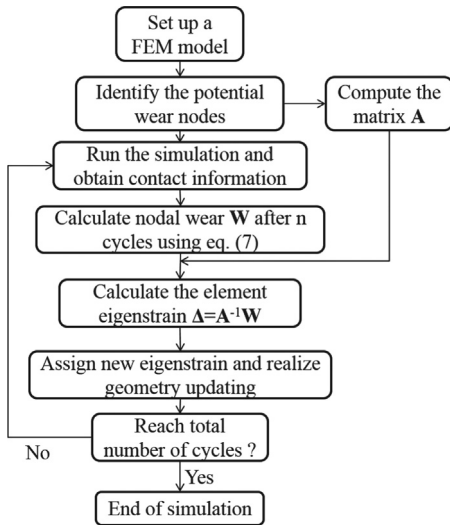
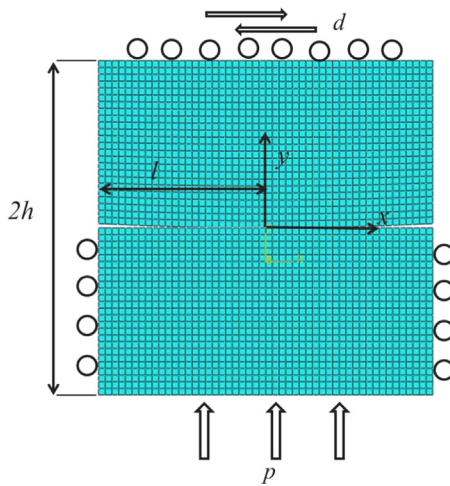**Fig. 2.** An Euler wear scheme based on the eigenstrain method.

Fig. 3. A 2D plane-strain wear model with boundary conditions of a constant compressive pressure, p, and an oscillating horizontal displacement, d. The indenter and substrate are elastically similar.

then updated through the inverse relation

$$\Delta = A^{-1} W. \tag{8}$$

This algorithm is shown as a block diagram in Fig. 2.

4. Validation and application in wear simulation

We implemented a two-dimensional ABAQUS model, using an anisotropic thermal expansion module to generate the eigenstrains, for the purpose of illustration, but the method is equally applicable for three-dimensional geometries, other finite-element packages, and other modules that represent eigenstrains. A round-on-flat sliding model was created, as shown in Fig. 3. A constant vertical pressure, p, was applied to the system as a preload. Then, an oscillating horizontal displacement, d, was applied to the top surface of the indenter. The amplitude of this displacement was chosen to be sufficient to cause slip at all nodes.

In this particular implementation, the eigenstrain vector, Δ was obtained by assigning negative temperatures, T_i to each contact nodes, corresponding to the appropriate eigenstrains through $\Delta_i = \alpha_T T_i$, where α_T is the coefficient of thermal expansion of the surface elements. All of the non-surface nodes were assigned zero

temperature, and the thermal conductivity was set to be zero, so that the temperature distribution remained unchanged. Obviously, this method cannot be used in problems involving actual thermo-elastic deformations, but in these cases the appropriate eigenstrains can be generated by alternative methods, such as anisotropic swelling modules.

Results for the wear profile and for the evolution of the contact pressure were obtained by two methods: (i) the thermal-contraction algorithm described above, and (ii) a conventional re-meshing algorithm. In the re-meshing algorithm, the contact nodes were relocated manually based on the predicted wear after n cycles and the original loading scenario was repeated. Since this procedure essentially involved unloading and then reloading the model after the geometry had been updated, the remeshed model was run for a few cycles until a steady cyclic state was identified. We note that ABAQUS contains an adaptive re-meshing module, but we encountered convergence problems when computing the contact interactions without the unloading and reloading step. Some of the calculations were also repeated using an anisotropic swelling module available in ABAQUS to confirm that non-thermal routes also work.

Fig. 4 shows the dimensionless wear profile after 100 and 200 stages of geometry modification, which corresponds to 100n and 200n loading cycles respectively. The values of the dimensionless parameters used were $\mu = 0.1, \alpha E = 0.0075, \nu = 0.25, d/l = 0.005$, $E/p = 3750$, and $h/l = 0.5$, where ν and E are Young's modulus and Poisson's ratio, respectively. The results of the thermal-expansion method are shown as circles and those of the re-meshing method as crosses. Clearly the two methods give essentially identical results. Similarly, the contact pressure predicted by the two methods is shown in Fig. 5. The percentage differences between the results of the two methods shown in Fig. 5 are slightly larger than that in Fig. 4, but the two sets of results are still not visually distinguishable. In all cases, the frictional tractions were proportional to the contact pressures, since slip occurred at all contact nodes. Results obtained using the anisotropic swelling module available in ABAQUS were indistinguishable from these results.

5. Discussion

In conventional re-meshing algorithms, it is generally necessary to unload the contact stress on the contact interface each time the geometry is updated. This is undesirable in problems involving plastic deformation, where unloading may lead to unintended modifications of the residual stress field. Also, in fretting problems, where frictional slip is restricted to a part of the contact interface, unloading will release residual frictional slip in the stick zone [17,18]. This necessitates running the model through several cycles to achieve a steady state after each mesh adjustment, and even
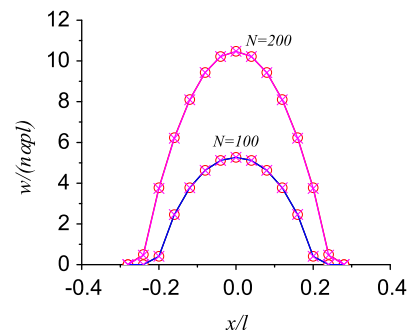

Fig. 4. Dimensionless wear profiles predicted by the thermal expansion algorithm (circles) and the re-meshing method (crosses) for the model shown in Fig. 3. N is the number of stages of geometry modification.
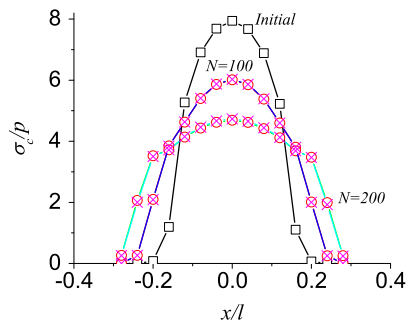
Fig. 5. The contact pressure predicted by the thermal expansion algorithm (circles) and the re-meshing method (crosses).

then, the release of residual slip may lead to accumulated errors. The adaptive-mesh module in ABAQUS appears to permit re-meshing without unloading and reloading, but the present authors' experience was that it could cause convergence problems.

By contrast, the example illustrated here shows that the eigen-strain algorithm generates the same solution as a conventional algorithm, without the need for unloading and reloading. This algorithm is considerably easier to implement than a re-meshing algorithm. It is also significantly more efficient. For example, in generating the results of Figs. 4 and 5, we found that the computer time with the new method was approximately one-third of that required for the conventional algorithm.

Although we used a simple two-dimensional model for the illustration in Section 4, the eigenstrain algorithm can also be applied to three-dimensional models. The method can also be extended using modifications previously introduced in re-meshing algorithms. For example, with modifications, it can be used to model large wear depths. If the wear depth is larger than a critical fraction of the element size [14,15], the geometry change can be distributed by defining eigenstrains over several layers of elements. We also note that other wear laws can be used in place of Eq. (4), provided that they depend only on quantities calculable from the underlying finite-element contact model.

6. Conclusions

The eigenstrain algorithm described in this paper provides an efficient and easy alternative to conventional re-meshing algorithms for finite-element simulations of contact problems involving wear. It enables wear modeling in commercial finite-element codes using available expansion modules. The method allows geometry updating, without the problems associated with unloading the contact stress at the interface interface. This provides advantages for history-dependent problems, such as those involving plasticity and/or hysteretic friction and microslip. Finally, we repeat the important point that, although, here, we used thermal expansion as an example of how to generate eigenstrains, the wear profile can also be mimicked by other available expansion modules, such as swelling. This approach releases the temperature field for use in thermal simulations, and so enables the application of this method to a broad range of thermo-tribological problems.

Acknowledgements

References

[1] Muts E-J, vanPelt H, Edelhoff D, Krejci I, Cune M. Tooth wear: a systematic review of treatment options. J Prosthet Dent, in press 2014;112(4):752–9 〈http://www.sciencedirect.com/science/article/pii/S0022391314000936〉.
[2] Mattei L, Di Puccio F, Piccigallo B, Ciulli E. Lubrication and wear modelling of artificial hip joints: a review. Tribol Int 2011;44(5):532–49 〈http://www.sciencedirect.com/science/article/pii/S0301679X10001647〉.
[3] Deuis R, Subramanian C, Yellup J. Dry sliding wear of aluminium composites-a review. Compos Sci Technol 1997;57(4):415–35 〈http://www.sciencedirect.com/science/article/pii/S0266353896001674〉.
[4] Gagg CR, Lewis PR. Wear as a product failure mechanism—overview and case studies. Eng Fail Anal 2007;14(8):1618–40 〈http://www.sciencedirect.com/science/article/pii/S1350630706002263〉.
[5] Hegadekatte V, Huber N, Kraft O. Finite element based simulation of dry sliding wear. Model Simul Mater Sci Eng 2005;13(1):57–75 〈http://iopscience.iop.org/0965-0393/13/1/005〉.
[6] Podra P, Andersson S. Simulating sliding wear with finite element method. Tribol Int 1999;32(2):71–81 〈http://www.sciencedirect.com/science/article/pii/S0301679X99000122〉.
[7] Soderberg A, Andersson S. Simulation of wear and contact pressure distribution at the pad-to-rotor interface in a disc brake using general purpose finite element analysis software. Wear 2009;267(12):2243–51 〈http://www.sciencedirect.com/science/article/pii/S0043164809005316〉.
[8] Mukras S, Kim NH, Sawyer WG, Jackson DB, Bergquist LW. Numerical integration schemes and parallel computation for wear prediction using finite element method. Wear 2009;266(7):822–31 〈http://www.sciencedirect.com/science/article/pii/S0043164808004286〉.
[9] McColl I, Ding J, Leen S. Finite element simulation and experimental validation of fretting wear. Wear 2004;256(11):1114–27 〈http://www.sciencedirect.com/science/article/pii/S0043164803005763〉.
[10] Archard JF. Contact and rubbing of flat surfaces. J Appl Phys 1953;24:981–8 〈http://dx.doi.org/10.1063/1.1721448〉.
[11] Menga N, Ciavarella M, Demelio G. An adaptive winkler model for a 2d hertzian wearing punch. In: 43rd national conference of the Italian association for stress analysis (AIAS); September 9–14, 2014. Rimini, Itlay.
[12] Park D, Kolivand M, Kahraman A. An approximate method to predict surface wear of hypoid gears using surface interpolation. Mech Mach Theory 2014;71:64–78 〈http://www.sciencedirect.com/science/article/pii/S0094114X1300178X〉.
[13] Oqvist M. Numerical simulations of mild wear using updated geometry with different step size approaches. Wear 2001;249(1):6–11 〈http://www.sciencedirect.com/science/article/pii/S0043164800005482〉.
[14] Rezaei A, Van Paepegem W, De Baets P, Ost W, Degrieck J. Adaptive finite element simulation of wear evolution in radial sliding bearings. Wear 2012;296(1):660–71 〈http://www.sciencedirect.com/science/article/pii/S0043164812002906〉.
[15] Tang L, Ding S, Xie Y, Huo Y. A multilayer nodes update method in fem simulation of large depth fretting wear. Wear 2013;301(1):483–90 〈http://www.sciencedirect.com/science/article/pii/S0043164812004668〉.
[16] Yeo T, Barber J. Finite element analysis of the stability of static thermoelastic contact. J Therm Stress. 1996;19(2):169–84 〈http://www.tandfonline.com/doi/abs/10.1080/01495739608946168〉.
[17] Churchman C, Hills D. General results for complete contacts subject to oscillatory shear. J Mech Phys Solids 2006;54(6):1186–205 〈http://www.sciencedirect.com/science/article/pii/S0022509606000020〉.
[18] Barber J, Davies M, Hills D. Frictional elastic contact with periodic loading. Int J Solids Struct 2011;48(13):2041–7 〈http://www.sciencedirect.com/science/article/pii/S0020768311001041〉.